Oscillatory interaction between synchronous generator and local voltage-dependent load

J.V. Milanović
I.A. Hiskens

Indexing terms: Synchronous generators, Oscillations, Stability, Static-load model

Abstract: The paper explores the influence of a voltage-dependent local load on electromechanical oscillations of a synchronous generator. The analysis is performed with different generator models, both with and without control devices. The classical static-load models were used as well as a generic model of dynamic load. It is shown that a voltage-dependent load can influence the damping of the electromechanical oscillations and thus the overall stability of the generator. This influence is very dependent on load parameters and on the generator's parameters and operating conditions. It is also shown that the use of dynamic-load models instead of static can have a significant influence on the evaluation of the total effect that voltage-dependent loads have on electromechanical oscillations of the generator.

1 Introduction

The problem of stability of synchronous generators has occupied the attention of the technical world for many years. The increase in unit sizes for steam generators above 1300 MW, and for hydro-electric generators above 900 MW for power-system-economics reasons, was possible only through an increase in current density in both stator and rotor. This is because all other parameters which contribute to the unit's apparent power increase have already reached limits determined by centrifugal forces, rotor sagging, rated frequency or saturation effects. The increase in current density and rated power is directly connected with an increase in per-unit reactances of the machine and a decrease in the inertia coefficient. This deterioration of parameters strongly affects small- and large-disturbance stability of generators. Significant effort has gone into overcoming the reductions in stability margin caused by these trends in machine design. The main method for compensation of parameter deterioration was, and still is, the use of different control devices. In previous studies, many aspects of the stability of generators have been discussed.

Appropriate settings of automatic-voltage-regulator parameters have been explored in search of improvements in damping and stability of synchronous generators [1]. Effects of power-system stabilisers [2, 3], static VAr compensators and control systems of HVDC links [4] have also been analysed, as these elements of power systems contribute greatly to stability and damping of the generator oscillations.

One of the main principles in all previous studies was how to damp electromechanical oscillations in generators. Electromechanical oscillations inevitably occur in multi-machine power systems. They result from rotors of machines oscillating with respect to one another. Oscillation energy is exchanged between machines through the transmission system [2]. These oscillations are called local mode if they occur between a single machine, or a small group of machines, and the rest of the system. Typical local-mode frequencies range from 0.7–2.0 Hz [5, 6]. Oscillations can also occur between large groups of machines. In that case they are called interarea oscillations, and typically have a frequency in the range from 0.1–0.8 Hz [5, 6].

Sustained oscillations in the power system are undesirable for many reasons. They can lead to fatigue of machine shafts, cause excessive wear of mechanical actuators of machine controllers and also make system operation more difficult. It therefore is desirable that oscillations are well damped.

Close attention has always been given to modelling of generators, with or without turbines, their associated controls, and transmission equipment. However the repesentation of loads has not traditionally been considered so thoroughly, even though it has been shown that loads can have a significant impact on analysis results [7–11]. The accurate modelling of loads is a difficult task for several reasons [12] such as: the large number of diverse load components, ownership and location of load devices in customer facilities that are not directly accessible to the electric utility, changing load composition with time of day and week, seasons and weather, lack of precise information on the composition of loads, and uncertainties regarding the characteristics of many load components.

One of the most significant effects of load on power-system behaviour is its influence on damping of power-system oscillations. In addition to the excitation controls, the inherent governor torque/speed characteristic and the generator amortisseurs, the load/frequency dependency was recognised as an important contributor to damping of system oscillations. This is especially important for interarea oscillations where the only sources of positive damping other than the generator excitation system are governor torque/speed and load/frequency characteristics because the effects of generator amortisseurs are mainly limited to local oscillations among nearby generators [13]. However, recently it has been shown that load-voltage dynamics can also have significant effects on

Paper 2120C (P7), first received 13th December 1994 and in revised form 30th May 1995

The authors are with the Department of Electrical and Computer Engineering, University of Newcastle, Callaghan, NSW 2308, Australia

damping [14–16]. In these studies only the active-power component of the load was treated as dynamic, while reactive power was modelled as a static function of voltage. The effects of both active and reactive-power dynamics on damping of oscillations are presented in [17] from the power-system point of view.

In this paper the effects of a nonlinear static and dynamic voltage-dependent load, connected at a generator's terminals, on damping of electromechanical oscillations and stability of the generator are presented. The effects are analysed with different, commonly used generators models, both with and without an exciter and governor. For a dynamic load, the effects of active-power and reactive-power dynamics, when taken into account separately and simultaneously, are also analysed.

2 Load modelling in power-system studies

Because of difficulties in defining actual load characteristics, utilities have attempted to use characteristics that would lead to conservative designs [8]. However, as a number of studies in the past have shown, there is no single load characteristic which leads to a conservative design for all system configurations [8]. The assumptions regarding the load model can influence predicted system behaviour as much as the models chosen for synchronous generators and associated controls.

2.1 Static-load models

Power-system-stability studies have traditionally used static-load models. Loads were represented as constant power, constant current or constant impedances, or in a general exponential form:

$$P(V) = P_o\left(\frac{V}{V_o}\right)^{n_{ps}} \tag{1}$$

$$Q(V) = Q_o\left(\frac{V}{V_o}\right)^{n_{qs}} \tag{2}$$

where P_o, Q_o and V_o are nominal active and reactive power and voltage of the bus, respectively. Coefficients n_{ps} and n_{qs} are voltage exponents for real and reactive power, respectively.

2.2 Aggregate dynamic-load models

Many measurements in different power systems around the world have been made to establish load models for different purposes. The form of response of different loads to a voltage step is given in a number of reports [11, 18–23]. It is of a general form shown in Fig. 1. The initial power step, the final power mismatch and the rate of recovery of the load are parameters which can vary greatly across different load types [7, 9, 12, 21]. A detailed mathematical model of the general form of exponential load response is given in [25].

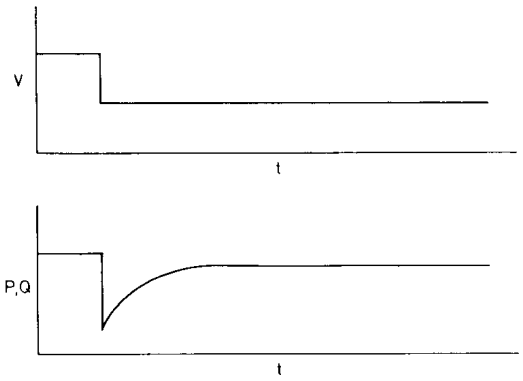

Fig. 1 *Typical load response to a step in voltage*

As explained in [21, 25] nonlinear voltage-dependent dynamic load can be represented in the form of a set of differential–algebraic equations as follows:

$$T_p\dot{x}_p = -x_p + P_s(V) - P_t(V) \tag{3}$$

$$P_d = x_p + P_t(V) \tag{4}$$

A similar aggregate-dynamic-load model was proposed in [26] in a form:

$$T_p\dot{x}_p = -x_p + P_s(V) - P_t(V) \tag{5}$$

$$P_d = x_p P_t(V) \tag{6}$$

In both previous models x_p is a state variable, P_d is the actual load demand, $P_s(V)$ and $P_t(V)$ are steady-state and transient load/voltage characteristics and T_p is a time constant which characterises the response of the load. The previous equations are for modelling active-power dynamics only, but reactive-power dynamics can be modelled in a similar way. It was shown in [27] that these two models can be tuned to have almost the same response to a step in voltage. However, they differ in terms of solvability of the differential–algebraic model.

In the sequel only the model given by eqns. 3 and 4 will be considered. The functions $P_s(V)$ and $P_t(V)$ can be defined as

$$P_s(V) = P_o\left(\frac{V}{V_o}\right)^{n_{ps}} \tag{7}$$

$$P_t(V) = P_o\left(\frac{V}{V_o}\right)^{n_{pt}} \tag{8}$$

where V_o and P_o are nominal voltage of the bus and the corresponding active power of the load, respectively, and n_{ps} and n_{pt} are steady-state and transient voltage exponents. Reactive-power functions are defined in a similar manner. Voltage exponents are generally in the ranges given in Table 1.

Table 1: Ranges of voltage exponents

Exponent	References
$0 \leqslant n_{ps} \leqslant 3$	7, 9, 12, 19, 21
$0 \leqslant n_{qs} \leqslant 7$	7, 9, 12, 19, 21
$1.5 \leqslant n_{pt} \leqslant 2.5$	21, 26
$4 \leqslant n_{qt} \leqslant 7$	21, 26

Time constants T_p and T_q, which characterise the recovery response of the load, can be chosen to represent different types of load. For industrial, agricultural and air-conditioning loads consisting predominantly of induction motors [8, 12, 13, 23], T_p and T_q are in the range of 0.02 s to a few seconds depending on the proportion of induction motors in the combined load. For responses of industrial plants such as aluminum smelters [24] or for power-plant-auxiliary system responses [22], they are in the range 0.1–0.5 s, while for tap changers and other control devices they are in the range of minutes. The time constants of heating load can be of the order of hours [21].

In [14], it was shown that linearisation of the load model of eqns. 3 and 4 yields

$$T_p\Delta\dot{x}_p = -\Delta x_p + \frac{P_o}{V_o}(n_{ps} - n_{pt})\Delta V \tag{9}$$

$$\Delta P_d = \Delta x_p + \frac{P_o}{V_o} n_{pt} \Delta V \tag{10}$$

This linearised model has the form of a lead/lag block, with the lead/lag time constants dependent on the load parameters. It was shown that, if $n_{pt} > n_{ps}$ ($n_{qt} > n_{qs}$), which is the normal situation, the phase shift through the real (reactive) load was always positive. The dependence on load parameters of the gain and phase shift of the load-transfer function was discussed in detail in [14].

3 Example system and analysis method

The simple system, given in Fig. 2, was used as a basis for exploration of the synchronous-generator–dynamic-load interaction. Third-order [15, 28, 29] and sixth-order [30–32] models of the synchronous generator were used.

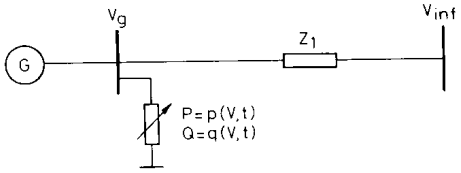

Fig. 2 *Single-machine infinite-bus system*

Local load was assumed to be voltage dependent, either in the form of the static-load model given by eqns. 1 and 2 or the dynamic load model given by eqns. 3 and 4 for active-power dynamics, with a similar model for reactive-power dynamics. The block diagrams of the governor, and of the exciter and power-system stabiliser are presented in Figs. 3 and 4, respectively. The complete model of this

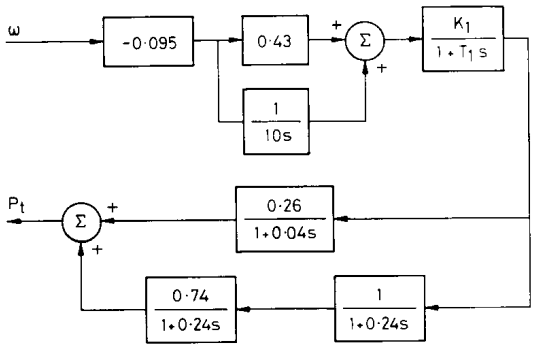

Fig. 3 *Block diagram of the governor and single-reheat steam turbine used in the study*

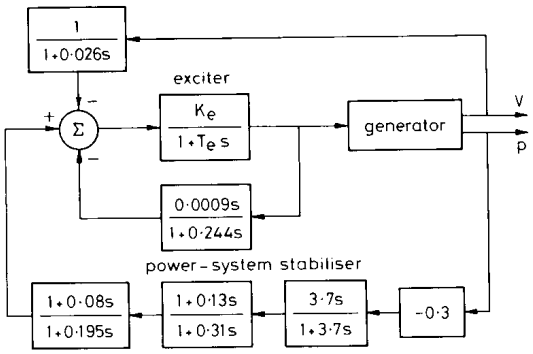

Fig. 4 *Block diagram of the exciter and power-system stabiliser used in the study*

system was linearised around the steady-state operating point. Small-disturbance stability analysis was used for evaluating stable or unstable operation and the level of damping of electromechanical oscillations.

Special software was developed for the purpose of analysing the effects of multiple dynamic loads in multimachine power systems. This investigation focused on the effects that variation of load-model parameters had on damping and frequency of electromechanical modes. The simple system of Fig. 2 only has one electromechanical mode. The complex conjugate pair of poles corresponding to this single electromechanical mode is dominant, i.e. the least damped poles for the range of load-model parameters which was of interest in this study. Hence the analysis was based on observing the effects that load-model-parameter variation had on this pair of poles. The more detailed description of building the state-space model of the system is given in [17].

4 Effects of voltage-dependent load

4.1 Differences between static and dynamic load effects

For the purpose of establishing the effects that the type of local load had on the damping of electromechanical oscillations, a sixth-order generator model was used. This model included a governor, automatic voltage regulator (AVR) and power-system stabiliser (PSS). Two general types of loads were used, namely static-exponential-load models and aggregate-dynamic-load models. In Fig. 5 the

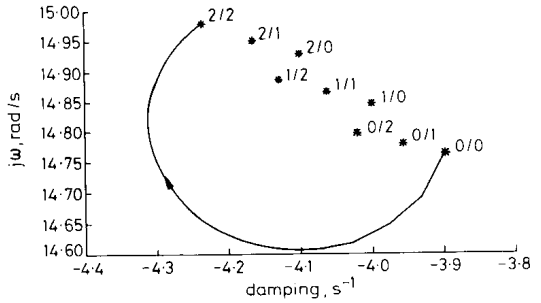

Fig. 5 *Static- and dynamic-load effects on damping of oscillations with control devices included*

stars mark the locations of the electromechanical mode when load was modelled by the exponential static model. The numbers beside the stars give the voltage exponents n_{ps}/n_{qs} used to determine each particular point. It can be seen that the worst case, from the point of view of damping, is constant power load. The best damping is achieved when load was modelled as a constant impedance. It is also noticeable that the increase in both active- and reactive-voltage exponents leads to better damped oscillations. However, the increase of the active-power voltage exponent has approximately twice the effect of an increase of the reactive power exponent.

It was concluded in [14] that, when the dynamic-load time constants T_p, T_q were very small, the load effectively behaved as a static load, with indices n_{ps}, n_{qs}. When T_p, T_q were very large, the load again behaved as a static load, but this time with indices n_{pt}, n_{qt}.

This effect is also shown in Fig. 5. In producing the root locus indicated by the solid line, time constants T_p, T_q were varied from 0 s, which is effectively static load, to 100 s. At the same time steady-state voltage-exponents n_{ps} and n_{qs} were fixed at 0 and transient-voltage exponents

n_{pt} and n_{qt} were fixed at 2. The arrow denotes movement of the electromechanical mode for time constant variation as mentioned. The root locus starts and finishes at the same points obtained with a static-load model with corresponding voltage exponents.

A similar effect is presented in Fig. 6. In this case the generator was considered alone, without any of the

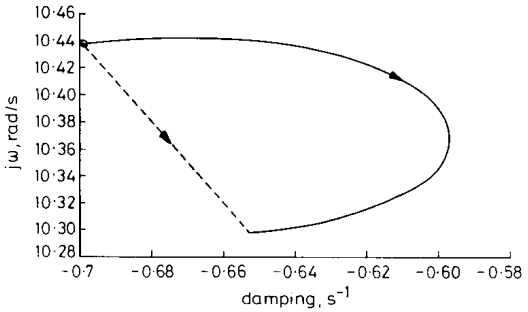

Fig. 6 *Static- and dynamic-load effects on damping of oscillations without control devices*

control devices. For the dynamic-load model, the time constants T_p, T_q were varied from 0 s to 100 s, and voltage exponents were fixed at $n_{ps} = 0.1$, $n_{qs} = 2$, $n_{pt} = 2.5$ and $n_{qt} = 5$. This root locus is presented as a solid line. For the static-load model, the voltage indices were varied from n_{ps}, n_{qs} to n_{pt}, n_{qt}. This is shown in Fig. 6 as a broken line. A small circle marks the location of the electromechanical mode when the static-load model was used, with indices of n_{ps}, n_{qs}. In these curves, the arrows denote the direction of movement of the mode as the time constants (for the dynamic load) and voltage exponents (for the static load) were varied as described.

As expected, the two curves start and finish at the same points. However they trace out significantly different paths. It can be seen that dynamic loads with time constants in the range from 0.1 s to a few seconds cannot be adequately described by a static representation. Note that this range of time constants corresponds to most dynamic loads, e.g. industrial and power-plant auxiliary power systems.

The differences in the shapes of the root loci for the two cases given by Figs. 5 and 6 can be explained by considering load/system interaction as shown in Fig. 7. This is discussed in detail in [14, 17].

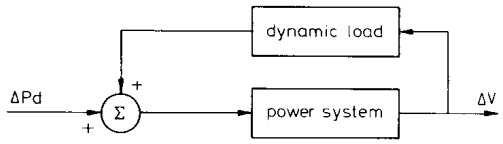

Fig. 7 *Power-system/dynamic-load interaction*

Basically, a disturbance in P_d, the power demand of a bus, will cause some variation in V, the load-bus voltage, as the system responds to the load disturbance, but variation of V will cause load to respond, resulting in variation of P_d. The phase difference between the input disturbance and the load variations, together with the gain through the load, will determine whether the load damps the disturbance or reinforces it. If the load variation is in phase with the P_d variation, the load will cause a decrease in damping. If load variation is 180° out of phase, the load will contribute to damping.

Bode plots of the system response, i.e. the frequency response of the feedforward block labelled 'power system' in Fig. 7, are given in Fig. 8. The Figure shows the two cases previously considered: the generator with and without controls. The average modal frequencies, from

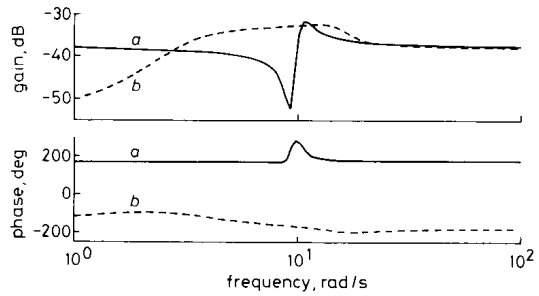

Fig. 8 *Bode plots for the system with and without control devices*
a Generator
b Generator + AVR + governor + PSS

Figs. 5 and 6, are 14.76 rad/s and 10.44 rad/s for the cases with and without control, respectively. From Fig. 8, it can be seen that the gain through the system for the two cases is about the same, i.e. approximately −32 dB. The phase shifts through the system at these resonant frequencies are completely different through, being −193.71° and 255.87°, respectively. This difference in phase shift is a major factor contributing to the difference in the shapes of the root loci.

For normal values of time constants and voltage exponents, the dynamic load always has a positive phase shift [17]. The amount of the phase shift depends on the load parameters. Consider first the case of the system with controls. Table 2 gives the load phase shift and

Table 2: Damping phase-shift dependence: case with controls

T_p, T_q	Load, phase shift	Open-loop phase shift	Damping
(s)	(deg)	(deg)	(1/s)
0.00	0.00	−193.71	−3.899
0.02	72.58	−123.13	−3.963
0.04	58.95	−134.76	−4.070
0.10	33.92	−159.79	−4.280
0.16	22.83	−179.89	−4.309
0.30	12.66	−181.05	−4.292
0.40	9.56	−184.15	−4.281
0.50	7.68	−186.03	−4.273
0.70	5.50	−188.21	−4.263
1.00	3.86	−189.85	−4.255

overall open-loop phase shift (the sum of the phase shifts through the system and the load), as well as system damping for increasing load time constant. These results confirm that as the open-loop phase shift approaches −180°, damping increases, then deteriorates again as the open-loop phase shift moves away from −180°. Note, though, that as the load time constant varies, so does the gain through the load. This has a secondary influence on the level of damping, and means that the system is not necessarily best damped when the load time constant gives a −180° phase shift.

Table 3 gives load phase shift, open-loop phase shift and damping for the second case, where the generator was without control devices. In this case it can be seen that the open-loop phase shift initially moves toward 360° as the load time constant increases from zero. Therefore a decrease in damping would be expected. This is consistent with the trend observed in Fig. 6. However, the variation in the gain through the system is now the dominant factor. Referring to Fig. 8, it can be seen that

Table 3: Damping phase shift dependence: case without controls

T_p, T_q	Load, phase shift	Open-loop phase shift	Damping
(s)	(deg)	(deg)	(1/s)
0.00	0.00	255.87	−0.6988
0.02	33.64	289.51	−0.6841
0.04	40.39	296.26	−0.6701
0.10	26.58	282.45	−0.6324
0.20	19.95	275.82	−0.6014
0.28	10.97	266.84	−0.5968
0.40	10.64	266.51	−0.6007
0.50	6.25	262.12	−0.6222
0.70	6.17	262.04	−0.6372
1.00	4.34	260.21	−0.6524

system gain is very sensitive to oscillation frequency. As the load time constant increases, the modal frequency changes a little, so the gain through the system will also vary. This example illustrates the complex nature of load/system interaction.

The higher gain over a wider range of frequency in the case with control devices contributes to higher sensitivity to load-parameter variation. The transfer function of the system without controls has a zero at 9.24 rad/s, which is close to the resonant frequency of 10.44 rad/s. This is shown clearly in Fig. 8. This zero is only effectively removed after inclusion of a PSS. Removal of this zero causes the significant change in phase shift through the system.

4.2 Effects of type of generator model

In some recent studies [15], a third-order machine model was used for studies of the effects of dynamic-load-model parameters on power-system damping. However, it has been found that the use of different generator models leads to different shapes of the root loci of the electromechanical mode as load-model parameters are varied. These differences are clearly evident in Fig. 9. In producing these root loci, control devices haven't been taken

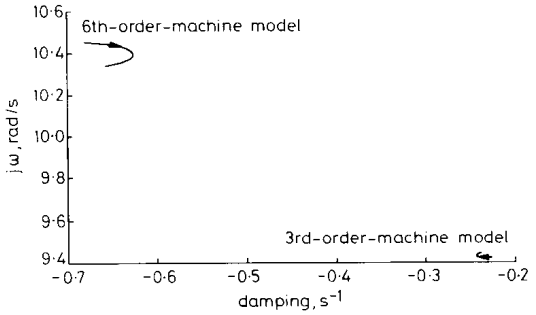

Fig. 9 *Root locus of electromechanical mode with different machine models for active power dynamics only*

into account. It can be seen that, with the higher-order machine model, which is a more accurate model, the effects of load dynamics are more pronounced. Note that the higher-order model is better damped because of the modelling of the generator's amortisseurs. As mentioned above, such differences can be explained by observing the frequency response of the system as seen from the bus where the dynamic load is connected. Recall that this is a frequency response of the feedforward block labelled 'power system' in Fig. 7. The input is the incremental change in bus power and the output is the change in bus voltage. These Bode plots are given in Fig. 10. It can be seen that, for the sixth-order machine model, the system has higher gain and the difference in phase shift between the two models is 162°. This difference in phase shift is largely due to a zero at 8.39 rad/s in the transfer function

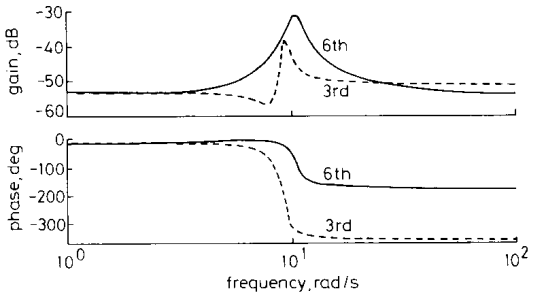

Fig. 10 *Bode plots for the system with different machine models for active power dynamics only*

obtained using the third-order machine model. This zero is close to the modal frequency of 9.24 rad/s. In the case of the sixth-order machine model, the zero is no longer present. This explains why load time constant variation leads to damping improvement in one case, and a deterioration in damping in the other.

From the point of view of the load time constants which provoke the best or worst damping, depending on the shape of the root locus, they are not altered significantly by the use of the more precise machine model. They are completely determined by load-model parameters and the resonant frequency of the modelled power system [14]. For the sixth-order machine model the power-system resonant frequency is 10.45 rad/s, and for the third-order machine model 9.43 rad/s. The corresponding critical time constants of the load are 0.14 s and 0.26 s, respectively. In all cases presented in this paper, the maximum effect on damping is achieved with time constants in the range 0.10–0.30 s.

4.3 Comparison of active and reactive-power dynamics

In all previous cases, both active and reactive power were treated as dynamic.

It has been shown [17] that there are differences in the effects that active and reactive power have on damping of interarea oscillations of a power system. These differences can be traced from the load model itself. In Fig. 11, step

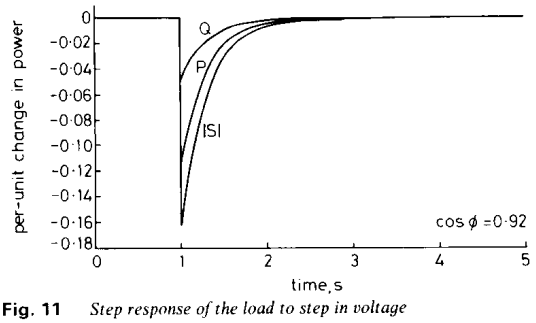

Fig. 11 *Step response of the load to step in voltage*

responses of the load to a step in voltage are shown when different components of load (active or reactive power, or both) were modelled as dynamic. In Fig. 12, Bode plots of gain and phase shift through the load are shown for different load dynamics. (These plots show the frequency response of the block labelled 'dynamic load' in Fig. 7.) Curves marked with a P indicate that only active power was modelled as dynamic, i.e. the Bode plot shows the

relationship between voltage and real power. Curves marked with a Q indicate that only reactive power was modelled as dynamic. The 'P and Q' corresponds to the

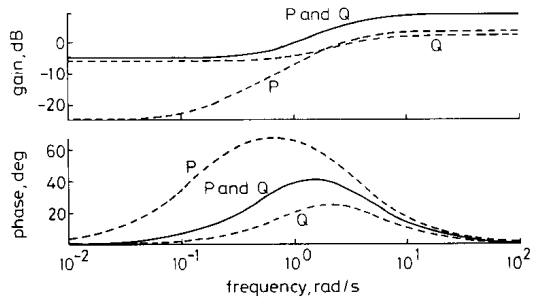

Fig. 12 *Bode plots of the gain and phase shift through the load when various components of apparent power are considered as dynamic*

Bode plot when both real and reactive power were dynamic. In this case the Bode plot shows the relationship between voltage and the output $|S| = \sqrt{(P^2 + Q^2)}$. Time constants $T_p = T_q = 0.3$ s were used, along with different voltage exponents of $n_{ps} = 0.1$, $n_{pt} = 2.5$, $n_{qs} = 2$ and $n_{qt} = 5$. It can be seen from Fig. 12 that the phase shift and the gain through the load are different for different types of load dynamics.

The effects of real- and reactive-power load dynamics on the damping of the electromechanical mode are presented in Fig. 13. The root loci correspond to variation of

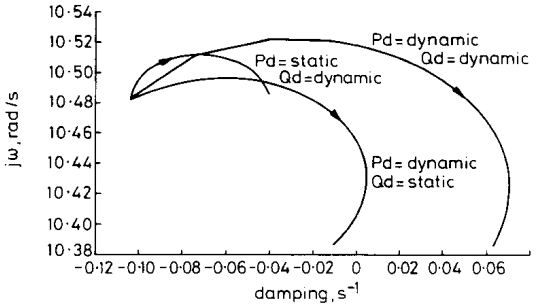

Fig. 13 *Root locus of electromechanical mode with different dynamics modelled*

time constants T_p and/or T_q from 0 s to 1 s. (When real power is modelled as dynamic, T_p is varied. With reactive power dynamic, T_q is varied. In the third case, when real and reactive power are both dynamic, T_p and T_q are varied equally.) It can be seen that active-power dynamics can cause a greater deterioration in damping than can the reactive-power dynamics. (This follows from the relative sizes of the loci.) When both real and reactive power are treated as dynamic, the deterioration of damping can be even more pronounced. For this particular choice of AVR and governor parameters, the system is stable when load is represented by the static model. (This corresponds to the starting point of all root loci.) If only the reactive power of the load has significant dynamics, damping deteriorates but the system remain stable. However, if active power exhibits a dynamic response, or if both active and reactive power together respond dynamically, then instability will result for a range of time constants.

4.4 Damping sensitivity to dynamic-model parameters

To gain a better understanding of the correspondence between values of load time constants and points on the root loci, one of the root loci of Fig. 13 is repeated in Fig. 14. The starting point in this Figure, denoted by 0, represents the static-load model. The region between points

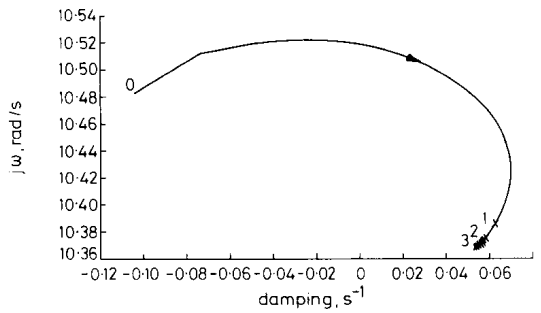

Fig. 14 *Root locus of electromechanical mode with different ranges of time constants marked*

0 and 1 (the point marked with the first small cross) was obtained by varying time constants T_p and T_q from 0 s–1 s. The worst damping occurred with time constants $T_p = T_q = 0.28$ s. The region between points 1 and 2 was obtained by varying time constants T_p and T_q over the range 1–10 s. Finally, the region between points 2 and 3 was obtained by varying time constants T_p and T_q over the range of 10–100 s. Note that points 2 and 3 almost overlap for the scaling used in Fig. 14. In all these cases steady-state active- and reactive-power voltage exponents n_{ps}, n_{qs} were equal to 0, and transient active- and reactive-power voltage exponents n_{pt}, n_{qt} were equal to 2.5. The governor and AVR were modelled. It was shown in [14] that, for frequencies in the range of 0.2–2 Hz, which are of interest in this study, the highest gains and phase shifts through the load, and hence the most significant effects of load dynamics, occur for load time constants up to 1 s. A more detailed explanation of the sensitivity of the load model to small values of time constants is given in [14].

Fig. 15 shows positions of the electromechanical mode when the parameters of the dynamic load were varied

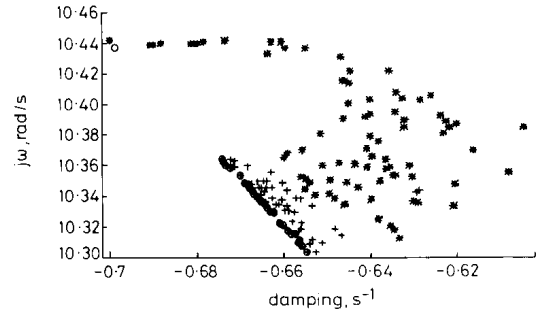

Fig. 15 *System damping when load parameters randomly chosen*

randomly. The values of n_{ps} and n_{qs} were held constant at 0.1 and 2, respectively, and no control devices were included. The following parameter ranges were used:

$$0 \leqslant T_p, \quad T_q \leqslant 100$$

$$1.5 \leqslant n_{pt} \leqslant 2.5$$

$$2 \leqslant n_{qt} \leqslant 5$$

In the Figure, the small circle shows the location of the electromechanical mode when load was represented statically. All other points correspond to dynamic loads. Note that the dynamic-load points cover quite a wide area. Stars represent variation of time constants in the

range 0–1 s, plus signs represent variation of time constants in the range 1–10 s, and encircled plus signs show variation of time constants in the range 10–100 s. Depending on load parameters, it is possible to have better or worse damping of the mode.

4.5 Influence of AVR and governor parameters

To determine which of the automatic-voltage-regulator and governor parameters are of most influence on the mode of interest, the participation matrix of the system was used. It has been found that those parameters are K_e and T_e for the AVR and K_1 and T_1 for the governor. These parameters are therefore shown in Figs. 3 and 4 as free parameters, while all others are fixed. The effects of their variation, together with load time constant variation in the range 0–1 s are presented in Figs. 16 and 17.

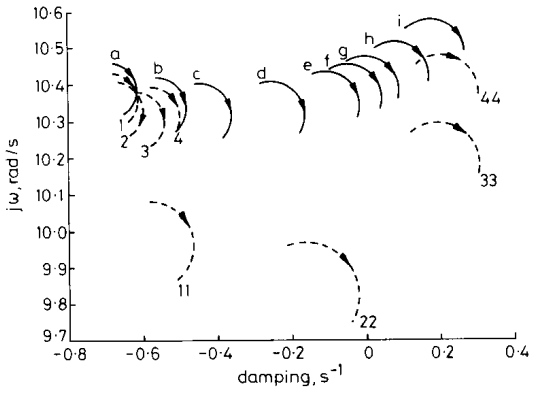

Fig. 16 *Effects of AVR parameters and load time constant variation*

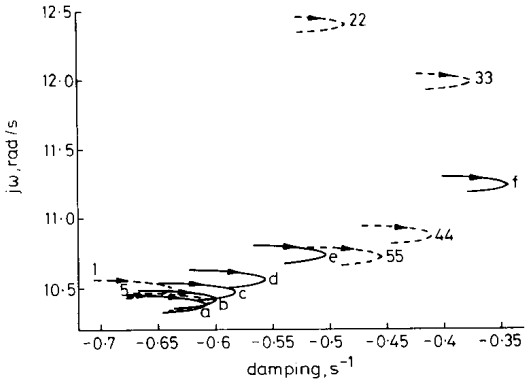

Fig. 17 *Effects of governor parameters and load time constant variation*

The following values of voltage exponents were used in producing the root loci: $n_{ps} = n_{qs} = 0$; $n_{pt} = n_{qt} = 2$. In both Figures, an *a* marks the root locus obtained when no control devices were connected to the generator.

In Fig. 16 the solid lines marked with the letters *b–i* are root loci for the following settings of AVR parameters: K_e = 30, 60, 120, 180, 210, 240, 300, 400; and T_e = 0.023 s. The broken lines present root loci for fixed K_e and different T_e for two cases: K_e = 30; T_e = 0.5 s, 0.25 s, 0.1 s, 0.05 s marked by 1, 2, 3, 4, respectively; and K_e = 400; T_e = 0.5 s, 0.25 s, 0.1 s, 0.05 s marked by 11, 22, 33, 44, respectively. It can be seen that, for different values of AVR parameters (especially for fast-acting AVRs), use of a dynamic load would indicate instability for certain values of time constants while a static-load model would indicate stable operation. In these investigations, it was assumed that PSS parameters were constant. The PSS was not retuned for the different values of AVR parameters, as the desire was to show the sensitivity to AVR parameters only.

In Fig. 17 the solid lines marked with the letters *b–f* are root loci for the following settings of governor parameters: K_1 = 0.2, 0.5, 1, 2, 5; and T_1 = 0.4 s. The broken lines present root loci for fixed K_1 and different T_1 for two cases: K_1 = 0.2; T_1 = 0.1 s, 1 s marked by 1, 5, respectively and K_1 = 5; T_1 = 0.15 s, 0.2 s, 0.7 s, 1 s, marked by 22, 33, 44, 55, respectively. It can be seen that, for different values of governor parameters, the electromechanical mode can be more or less damped.

From Figs. 16 and 17, it can be concluded that different values of parameters of generator control devices, if within standard ranges, do not alter the general shape of the root loci. (Recall though, from Fig. 8 that the addition of controls, in particular a PSS, could have a major effect on the shape.) It is possible, however, that, for certain controller parameter settings, the system may be stable or unstable, depending on dynamic-load parameters.

4.6 Influence of the impedance between generator and load

The results of the previous Sections have been based on the power system shown in Fig. 2. In that system the load is at the generator bus. However, we now wish to see how results change when the load is supplied from a bus which is not the generator bus. The effect on damping of the impedances between the generator, the infinite bus and the load is shown in Fig. 18. Variation of these

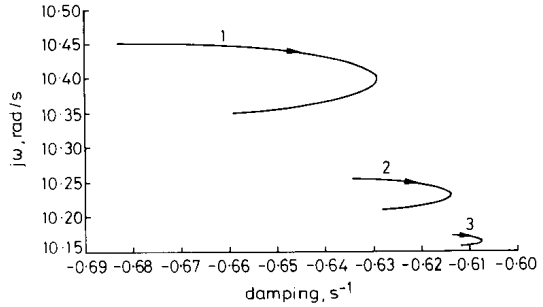

Fig. 18 *Effects of impedance between generator and load*

impedances does not alter the shape of the root loci, but does affect the overall sensitivity of damping to load parameters. The loci shrink, i.e. sensitivity reduces, as the impedance between the generator and the load bus grows, and the impedance between the load bus and the infinite bus decreases (the load bus moves closer to the infinite bus). Referring to Fig. 18, the loci follow the sequence $1 \rightarrow 2 \rightarrow 3$. This can be explained by the fact that, with a decrease in impedance between the load and the infinite bus, the voltage at the load bus becomes more rigid, i.e. the variation in voltage is less, so ultimately the effect of the voltage dependent load is reduced.

Note though that, as the load moves towards the infinite bus, the overall level of damping reduces. This behaviour can be explained by considering the system power flows. At steady state, the generator produces 0.9 p.u. real power, and the load absorbs 0.6 p.u. real power. In the situation with the load at the generator bus, real power flow over the line between the generator

and the infinite bus is 0.3 p.u. As the load bus is moved toward the infinite bus, the section of line between the generator and load carries 0.9 p.u., so the transmission line becomes more heavily loaded. It follows from classical analysis that damping will decrease.

5 Conclusions

A standard static-load model and a generic nonlinear-dynamic-load model have been used to investigate the influence of load on the damping of the electromechanical oscillations of a generator, and thus on its stability.

The paper shows that loads which respond dynamically to voltage variations can have an influence on the stability of generators by affecting the damping of electromechanical modes. It is shown that, depending on load and system parameters, a dynamic load can reinforce oscillations, and so cause a deterioration in damping and stability. It is also possible, though, that the load may oscillate out of phase with the system, and so lead to an improvement in damping.

Use of different-order machine models may lead to different results as far as the effects of load dynamics on damping are concerned. This indicates that, by using simpler models of synchronous machines, incorrect conclusions could be drawn regarding the effects of load on damping and stability.

The nature of the influence of load dynamics on the stability of the generator is not changed by the inclusion of exciters and governors. All these components, in the cases examined (without retuning of the PSS), contributed mainly to a deterioration in damping. It was possible to find cases which were stable for certain sets of load model parameters, e.g. static load, but unstable for others.

The study has demonstrated the need for accurate modelling of loads. A static representation of loads that in reality exhibit significant dynamic behaviour can give very misleading results.

The significance of load-model uncertainty was considered. To do this, load parameters were randomly varied, with damping being determined for each set of parameters. This study indicated that the calculated values of damping could be quite widespread.

6 References

1 DEMELLO, F.P., and CONCORDIA, C.: 'Concepts of synchronous machine stability as affected by excitation control', *IEEE Trans.*, 1969, **PAS-88,** (4), pp. 189–202

2 LARSEN, E.V.: 'Applying power system stabilisers', *IEEE Trans.*, 1981, **PAS-100,** pp. 3010–3046

3 WANG, H.F., HAO, Y.S., HOGG, B.W., and YANG, Y.H.: 'Stabilization of power systems by governor-turbine control', *Int. J. Elect. Power Energy Syst.*, 1993, **15,** (6), pp. 351–361

4 WANG, L.: 'A comparative study of damping schemes on damping generator oscillations', *IEEE Trans.*, 1993, **PWRS-8,** (2), pp. 613–619

5 VERGHESE, G.C., PÉREZ-ARRIAGA, I.J., and SCHWEPPE, F.C.: 'Selective modal analysis with applications to electric power systems. Part II: The dynamic stability problem', *IEEE Trans.*, 1982, **PAS-101,** (9), pp. 3126–3134

6 KLEIN, M., ROGERS, G.J., and KUNDUR, P.: 'A fundamental study of inter-area oscillations in power systems', *IEEE Trans.*, 1991, **PWRS-6,** (3), pp. 914–921

7 CRAVEN, R.H., and MICHAEL, M.R.: 'Load representations in the dynamic simulation of the Queensland power system', *J. Elect. Electron. Eng.*, 1983, **3,** (1), pp. 1–7

8 KENT, M.H., SCHMUS, W.R., McCRACKIN, F.A., and WHEELER, L.M.: 'Dynamic modelling of loads in stability studies', *IEEE Trans.*, 1969, **PAS-88,** (5), pp. 756–763

9 RAO, N.D., and TRIPATHY, S.C.: 'Effects of load characteristics and voltage-regulator speed-stabilizing signal on power system dynamic stability', *Proc. IEE*, 1977, **124,** (7), pp. 613–618

10 MAURICIO, W., and SEMLYEN, A.: 'Effect of load characteristics on the dynamic stability of power systems', *IEEE Trans.*, 1972, **PAS-91,** pp. 2295–2304

11 LIN, C.-J., CHEN, V.-T., CHIOU, C.-Y., HUANG, C.-H., CHIANG, H.-D., WANG, J.-C., and FEKIH-AHMED, L.: 'Dynamic load models in power systems using the measurement approach', *IEEE Trans.*, 1993, **PWRS-8,** (1), pp. 309–315

12 IEEE TASK FORCE: 'Load representation for dynamic performance analysis', *IEEE Trans.*, 1993, **PWRS-8,** (2), pp. 472–482

13 CONCORDIA, C., and IHARA, S.: 'Load repesentation in power system stability studies', *IEEE Trans.*, 1982, **PAS-101,** (4), pp. 969–977

14 MILANOVIĆ, J.V., and HISKENS, I.A.: 'Effects of load dynamics on power system damping'. IEEE/PES Summer Meeting, San Francisco, USA, 1994, paper 94 SM 578-5 PWRS (to appear IEEE Transactions on Power Systems)

15 MILANOVIĆ, J.V., and HISKENS, I.A.: 'Effects of dynamic load model parameters on damping of oscillations in power system', *Elect. Power Syst. Res.*, 1995, **33,** (1), pp. 53–61

16 MILANOVIC, J.V., and HISKENS, I.A.: 'The effects of dynamic load on steady state stability of synchronous generator', Proceedings of the international conference on Electrical Machines, ICEM'94, Paris, September 1994, Vol. 2, pp. 722–727

17 HISKENS, I.A., and MILANOVIĆ, J.V.: 'Load modelling in studies of power system damping'. IEEE/PES Winter Meeting, New York, 1995, paper 95 WM 111-5 PWRS (to appear in IEEE Transactions on Power Systems)

18 PRICE, W.W., WIRGAU, K.A., MURDOCH, A., MITSCHE, J.V., VAAHEDI, E., and EL-KADY, M.A.: 'Load modelling for power flow and transient stability computer studies', *IEEE Trans.*, 1985, **PWRS-3,** (1), pp. 180–187

19 SABIR, S.A.Y., and LEE, D.C.: 'Dynamic load models derived from data acquired during system transients', *IEEE Trans.*, 1982, **PAS-101,** (9), pp. 3365–3372

20 WELFONDER, E., WEBER, H., and HALL, B.: 'Investigations of the frequency and voltage dependence of load part systems using a digital self-acting measuring and identification system', *IEEE Trans.*, 1989, **PWRS-4,** (1), pp. 19–25

21 KARLSSON, D., and HILL, D.J.: 'Modeling and identification of nonlinear dynamic loads in power systems', *IEEE Trans.*, 1994, **PWRS-9,** (1), pp. 157–166

22 SHACKSHAFT, C., SYMONS, O.C., and HADWICK, J.G.: 'General-purpose model for power-system loads', *Proc. IEE*, 1977, **124,** (8), pp. 715–723

23 OHYAMA, T.: 'Voltage dependence of composite loads in power systems', *IEEE Trans.*, 1985, **PAS-104,** (11), pp. 3064–3073

24 ARNOLD, C.P., TURNER, K.S., and ARRILLAGA, J.: 'Modelling rectifier loads for a multi-machine transient-stability programme', *IEEE Trans.*, 1980, **PAS-99,** (1), pp. 78–85

25 HILL, D.J.: 'Nonlinear dynamic load models with recovery for voltage stability studies', *IEEE Trans.*, 1993, **PWRS-8,** (1), pp. 166–176

26 XU, W., and MANSOUR, Y.: 'Voltage stability analysis using generic dynamic load models', *IEEE Trans.*, 1994, **PWRS-9,** (1), pp. 479–493

27 HISKENS, I.A., and HILL, D.J.: 'Modelling of dynamic load behaviour'. Proceedings of NSF/ECC workshop on Bulk Power System Voltage Phenomena III, Davos, Switzerland, 1994

28 HEFFRON, W.G., and PHILLIPS, R.A.: 'Effect of a modern voltage regulator on underexcited operation of large turbine generators', *AIEE Trans.*, 1952, **71,** pp. 692–697

29 VOURNAS, C.D., and FLEMING, R.J., 'Generalization of the Heffron–Phillips model of a synchronous generator', IEEE PES Summer Meeting, Los Angeles, 1978

30 HAMMONS, T.J., and WINNING, D.J.: 'Comparisons of synchronous machine models in the study of the transient behaviour of electrical power systems', *Proc. IEE*, 1971, **118,** (10), pp. 1442–1458

31 HAMMONS, T.J., and CANAY, I.M.: 'Effects of damping modelling and the clearing process on response torque and stressing of turbine-generator shaft', *IEEE Trans.*, 1986, **EC-1,** (1), pp. 113–121

32 KRAUSE, P.C.: 'Analysis of electric machinery' (McGraw-Hill Book Co., New York, 1986)